Chapter 9
Turbulence in the Plasma: Self-organized Criticality and Its Local Breakdown

Turbulent transport is at the frontier of plasma confinement research and is still under development. Here, the basic concepts of the dynamical system are introduced as a useful fundamental discipline. Thermal diffusion of the low confinement state can be explained by the self-organized criticality examined by complexity science and the transport barrier is formed by the local breakdown of self-organized criticality when a turbulent cell is torn by the flow shear.

9.1 Concepts of Nonlinear Dynamics: Dynamical System and Attractor

The concept of "attractor" in the dynamical system is useful in understanding the turbulence generated in high temperature plasma. A system evolving according to the deterministic law is called a "dynamical system." The motion of the dynamical system is expressed in the phase space, which consists of the variables of the equation of motion. Even if the system is not related to physical dynamics, it is still called a dynamical system if the state follows the deterministic law. A dynamical system with some conserved quantity is called a "conservative system," while a system with some quantity being dissipated is called a "dissipative system." The motion of a dissipative system settles down to a specific trajectory or point in time. The stable state after the transition is called the attractor. There are four types of attractors (Figure 9.1):

1. Equilibrium point: the motion converges to a point in phase space.
2. Limit cycle: repeat the periodic motion in phase space.
3. Torus: Motion in phase space around the torus.
4. Chaotic attractor: phase space orbit never closes.

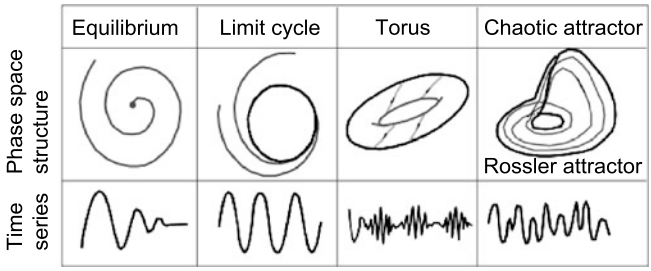

Figure 9.1 Phase space structures and time waveforms of attractors in the dynamical system

Even in the following simple linear oscillation system, the motion around the equilibrium point shows interesting variations in the parameter space (b, c), [1] (Figure 9.2).

$$\frac{\mathrm{d}^2X}{\mathrm{d}t^2} + b\frac{\mathrm{d}X}{\mathrm{d}t} + cX = 0\,. \tag{9.1}$$

The phase diagram $(X, \dot{X})$ of this system has a saddle point at $(0, 0)$ (unstable equilibrium point) in the case where $c < 0$ and the damping term $b = 0$. Adding the nonlinear term $eX^3 (e > 0)$ to above equation, two equilibrium points (point attractors) appear at $X = \pm(-c/e)^{1/2}$ and motion around each one and encircling the two develops. If the damping term is added, the system converges asymptotically toward one of equilibrium points. Addition of the nonlinear term $e(\mathrm{d}X/\mathrm{d}t)^3$ also produces the limit cycle in the region $c > 0, b < 0$. Negative linear damping $(b < 0)$ produces an outward spiral orbit from $(0, 0)$ and reaches a stable limit cycle orbit dominated by the nonlinear term. In the planar phase space, the equilibrium and the limit cycle are the only two final states of the dynamical system. This comes from the simple fact that the plane is divided into an inner region and an outer region by a closed curve.

An important 2-dimensional phase space structure that differs from the planar phase space is the torus. A torus naturally occurs due to the forced vibration when the external force acts on the system. There are two quasi-periodic motions caused by the two low frequencies. Such a system is structurally unstable for small perturbations by the frequency locking when the ratio of two frequencies becomes an integer.

The stability of the equilibrium point can be described by "Lyapunov stability," mentioned in Section 6.1. According to Lyapunov, a system is stable if the neighborhood of the equilibrium remains as the neighborhood forever. The system is called "asymptotically stable" if the solution converges to an equilibrium point as $t \to \infty$. The system is said to be "structurally stable" when the topology of the flow does not change when a small perturbation is applied.

When a system parameter μ changes, the eigenvalue of the linearized evolution equation $\dot{\boldsymbol{x}} = F(\boldsymbol{x}, \mu)$ draw a trajectory in the complex plane. If the eigenvalue stays in the left half of the plane for $\mu = \mu_0$, "bifurcation" occurs when the eigenvalue crosses the imaginary axis.

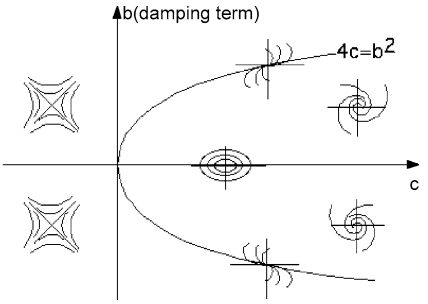

Figure 9.2 Phase-space structure on the parameter space (c, b) for the linear dynamic system Equation 9.1

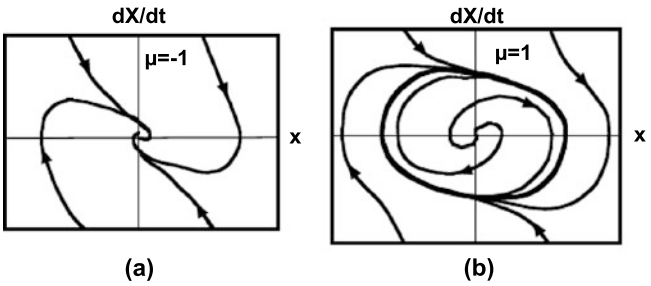

Figure 9.3 Phase diagrams of Equation 9.2 (a) before ($\mu = -1$) and (b) after ($\mu = 1$) Hopf bifurcation. The case of $\mu = 1$ is the limit cycle

If the system has only one eigenvalue, it moves along the real axis. Bifurcation occurs when one crosses the imaginary axis and is called "fold bifurcation." Fold bifurcation is a structurally stable bifurcation. If the system has two eigenvalues, they are complex conjugate and the bifurcation occurs when they cross the imaginary axis; this bifurcation is called "Hopf bifurcation." As an example of Hopf bifurcation, consider the following nonlinear damped oscillation system:

$$\frac{\mathrm{d}^2 X}{\mathrm{d}t^2} - \mu \frac{\mathrm{d}X}{\mathrm{d}t} + X + \left(\frac{\mathrm{d}X}{\mathrm{d}t}\right)^3 = 0\,. \tag{9.2}$$

The origin is asymptotically stable when $\mu < -2$ and is a stable spiral when $-2 < \mu < 0$. Furthermore, the origin is an unstable spiral when $0 < \mu$ and the flow is attracted by the newly formed limit cycle (see Figure 9.3).

9.2 Self-organized Criticality: Turbulent Transport and Critical Temperature Gradient

The study of heat transport across magnetic surfaces has been ongoing since the start of the fusion research. But, mechanisms governing the process have not been

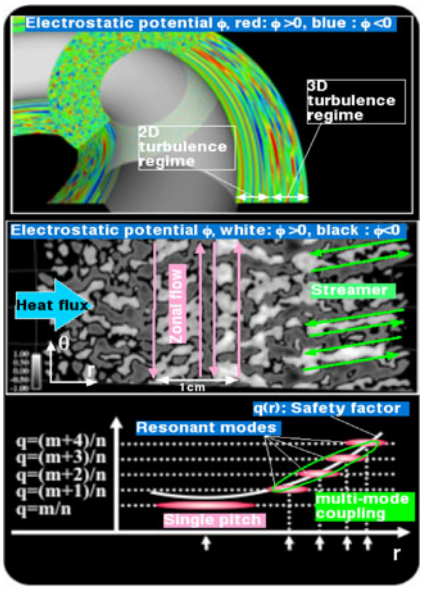

Figure 9.4 Variation of the spatial structure of turbulence with magnetic shear in the electron channel [2]. In the low shear regime, zonal flow is formed by the inverse cascade of 2-dimensional turbulence. In the finite shear regime, streamer is formed due to radial mode coupling

fully clarified since turbulent transport in plasma is a complex and nonlinear process. In recent years, fundamental processes have been elucidated since zonal flow and streamers produced by the wave–wave interaction is clarified through the gyrokinetic and gyrofluid simulations. The existence of the critical temperature gradient (see Section 7.5) has also been shown by experiments using localized electron cyclotron heating.

In plasma confined in a closed magnetic configuration, a large spatial temperature gradient occurs since the plasma core is heated to a few 100 million degrees while the temperature at the boundary of the closed magnetic field is low enough (but still a few million degrees). In high-temperature plasma, the ion temperature gradient drift wave mentioned in Section 7.5 (ITG-drift wave), electron temperature gradient drift wave (ETG-drift wave), and trapped electron mode (TEM) can be unstable. These modes become unstable when the temperature gradient exceeds a critical temperature gradient $(\mathrm{d}T/\mathrm{d}r)_\mathrm{c}$ similar to the case of thermal convection (see Salon 1). This is called the "critical temperature gradient."

An interesting observation in the gyrokinetic simulation of ETG turbulence [2] is that the structure of the turbulence is strongly dependent on magnetic shear as shown in Figure 9.4). In the zero magnetic shear regime (regime around q_min in the negative magnetic shear configuration), plasma turbulence has a 2-dimensional structure as described by the Hasegawa–Mima equations in Section 7.3 and excites zonal flow by the inverse cascade of the turbulent spectrum [3]. Meanwhile, a radially stretched "streamer" is created through radial mode coupling and intermittent heat transport is produced in the positive shear region. This situation is exactly the same as avalanches of sand piles.

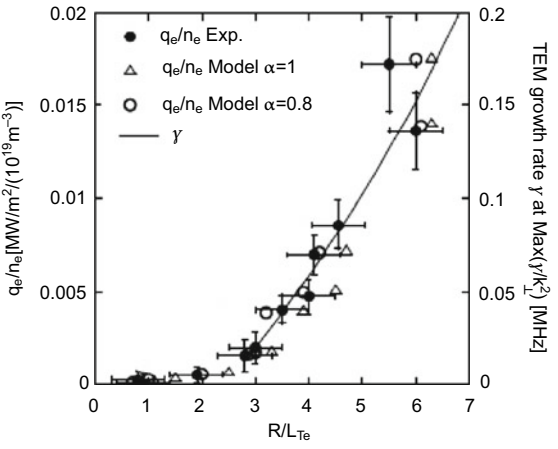

Figure 9.5 Experimental verification of critical temperature gradient transport in a tokamak in (R/L_{Te}, q_e/n_e) plane [4]. At low R/L_{Te}, heat flux is quite small indicating that ETG turbulence is suppressed, while ETG turbulence grows at high R/L_{Te} [4]

In the electron channel, the ETG-drift wave becomes unstable if the electron temperature is close to or lower than the ion temperature, while TEM becomes unstable if the electron temperature is higher than the ion temperature. Figure 9.5 shows experimental observations of electron heat transport [4]. There is a critical temperature gradient $R/L_{Te} \sim 2.5$ ($L_{Te} = -T_e/\mathrm{d}T_e/\mathrm{d}r$) and transport is very small in $R/L_{Te} < 2.5$, while the transport rate grows rapidly in $R/L_{Te} > 2.5$.

Note: Dissipative Structure and Bernard Convective Cell

A closed magnetic configuration for controlled fusion is a "closed system" in terms of equilibrium but is an "open system" in terms of heat. In the closed system, the equilibrium structure is determined in line with thermal equilibrium. On the other hand, the open system can maintain an off-equilibrium state as long as a driving force exists. The various shapes and motions arising from the driving force of open systems are named "dissipative structures" by I. Prigogine [5]. As a typical example, he uses "Bernard cells." In thermal convection under gravity, the system becomes linearly unstable when a non-dimensional "Rayleigh number" R related to the temperature difference ΔT exceeds a critical value R_c and a convective cell structure appears [6]:

$$\frac{\partial u}{\partial t} + \frac{1}{P_r}(u \cdot \nabla u) = -\frac{1}{P_r}\nabla p + \nabla^2 u + RkT \ , \tag{9.3}$$

$$P_r \frac{\partial T}{\partial t} + (u \cdot \nabla)T = \nabla^2 T \nabla \cdot u = 0 \ . \tag{9.4}$$

Here, $R = (g\alpha d^4/\kappa\nu)|\Delta T/\Delta z|$ is the Rayleigh number, $P_\mathrm{r} = \kappa/\nu$ is the Prandtl number, g gravitational acceleration, α thermal expansion coefficient, κ thermal conductivity, ν dynamic viscosity, d the vertical thickness, and $\Delta T/\Delta z = (T_1 - T_2)/d$.

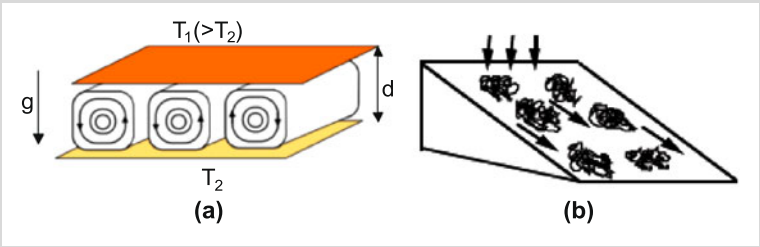

Figure 9.6 (a) Bernard convective cell as dissipative structure and (b) sand pile as self-organized criticality

Critical Phenomena and Self-organized Criticality

Critical phenomena are observed in the phase transition of thermal equilibrium, for example, the paramagnetic-ferromagnetic transition in magnetism. Magnetization defined in the crystal lattice u_j is given by $u_j = 0$ at $T > T_c$ and $u_j = a(T - T_c)$ at $T < T_c$. The spatial correlation length of the magnetization is $\sim 1/\kappa$, while $\kappa = \kappa_0((T - T_c)/T_c)^{1/2}$ and is divergent if $T \to T_c$. Namely, the effect of fluctuation in the critical state extends over a long distance. The statistical physics tells us that fluctuation in thermal equilibrium follows a Gaussian distribution. If you check the process that leads to the Gaussian from a random walk, it can be seen that Gaussian distribution $P(x) = \exp(-bx^2)$ is a special case.

The power law $P(x) = x^{-n}$ frequently appears in non-equilibrium open systems. Sand pile avalanches occur when the sand pile reaches a certain critical slope and the relation between the magnitude and frequency is given by the power law x^{-2}. Per Bak (1948–2002) [7] called this state as "self-organized criticality." The frequency and scale of earthquakes (relation between magnitude M and frequency (occurrence/year) of earthquakes above M) follows the famous Gutenberg–Richter law f^{β} ($\beta \sim 0.94$).

9.3 Chaotic Attractor: Three-wave Interaction in Drift Wave Turbulence

As mentioned in Section 7.3, drift wave turbulence can be regarded as the result of many three-wave interactions. Plasma turbulence is a natural (or settled) state with oscillations due to nonlinear processes rather than growing instability. It is important to examine the phase space structure to understand its behavior. The saturated state of plasma turbulence dominated by the three-wave interaction has a "chaotic attractor" structure. Fourier expansion of the electrostatic potential is given by

$$\tilde{\Phi}(\boldsymbol{x}, t) = \sum_{\boldsymbol{k}} \tilde{\Phi}_{\boldsymbol{k}}(t) \exp(\mathrm{i}\boldsymbol{k} \cdot \boldsymbol{x}) \ . \tag{9.5}$$

Then, the nonlinearity is given by the interaction of the wave with wave number $\boldsymbol{k}_1$ and $\boldsymbol{k}_2$ as follows,

$$\boldsymbol{k} = \boldsymbol{k}_1 + \boldsymbol{k}_2 \ . \tag{9.6}$$

Although $k_{//} \neq 0$ is assumed, the Hasegawa–Mima equation 7.80 is essentially 2-dimensional turbulence and can be rewritten by transforming $\boldsymbol{k}_\perp \to \nabla_\perp$ as follows,

$$(1 - \rho_s^2 \nabla^2) \frac{\partial \tilde{\Phi}}{\partial t} + v_{de} \frac{\partial \tilde{\Phi}}{\partial y} - \left[\tilde{\Phi}, \rho_s^2 \nabla^2 \tilde{\Phi}\right] = 0 \tag{9.7}$$

$$\rho_s^2 = \frac{m_i T_e}{e^2 B^2} \ , \quad \left[\tilde{\Phi}, \tilde{\Psi}\right] = \boldsymbol{e}_z \cdot \nabla \tilde{\Phi} \times \nabla \tilde{\Psi} \ . \tag{9.8}$$

The adiabatic response (Boltzmann distribution) for electrons (Equation 7.68) is assumed in the Hasegawa–Mima equation and is an essentially conservative system. The mass $\mathcal{M}$, energy $\mathcal{W}$, and potential enstrophy $\mathcal{U}$ of the turbulence are conserved [8].

$$\mathcal{M} = \int \left[\tilde{\Phi} - \rho_s^2 \nabla_\perp^2 \tilde{\Phi}\right] \mathrm{d}x \mathrm{d}y \ , \tag{9.9}$$

$$W = \frac{1}{2} \int \left[\tilde{\Phi}^2 + \rho_s^2 \left(\nabla_\perp \tilde{\Phi}\right)^2\right] \mathrm{d}x \mathrm{d}y \ , \tag{9.10}$$

$$U = \frac{1}{2} \int \left[\left(\nabla_\perp \tilde{\Phi}\right)^2 - \rho_s^2 \left(\nabla_\perp^2 \tilde{\Phi}\right)^2\right] \mathrm{d}x \mathrm{d}y \ . \tag{9.11}$$

The 2-dimensional turbulence equation with dissipation is given by Hasegawa–Wakatani [9]. Here, we show this effect according to Horton–Ichikawa [10]. Two-dimensional drift wave turbulence including dissipation is expressed by adding a dissipation term to the Hasegawa–Mima equation (9.7).

$$(1 + L) \frac{\partial \tilde{\Phi}}{\partial t} + v_{de} \frac{\partial \tilde{\Phi}}{\partial y} + \hat{\gamma}_i \tilde{\Phi} + \left[\tilde{\Phi}, L\tilde{\Phi}\right] = 0 \tag{9.12}$$

$$L = L_h + L_{ah} = -\rho_s^2 \nabla^2 + \delta_0 (c_0 + \rho_s^2 \nabla^2) \frac{\partial}{\partial y} \ .$$

Here, $\hat{\gamma}_i$ is the ion Landau damping and the wave decay rate by the coupling to the decay wave. $L_h = -\rho_s^2 \nabla^2$ is the Hermitian operator, and the effect of dissipation is given by the non-Hermitian operator $L_{ah} = \delta_0 (c_0 + \rho_s^2 \nabla^2) \partial / \partial y$.

We introduce the electrostatic potentials of interacting three-drift waves $\varphi_j(t) = \varphi_{\boldsymbol{k}_j}(t)$ $(j = 1, 2, 3)$ by using amplitude a_j and phase ζ_j as follows,

$$(1 + k_j^2)^{1/2} \varphi_{\boldsymbol{k}_j}(t) = a_j(t) \exp[i \zeta_j(t)] \ . \tag{9.13}$$

Then, the following equations for three-wave amplitudes a_1, a_2, a_3 and total phase $\zeta = \zeta_1 + \zeta_2 + \zeta_3$ can be obtained for (j, k, l) 3 wave interaction.

$$\frac{\mathrm{d}a_j(t)}{\mathrm{d}t} = \gamma_j a_j - A a_k a_l (F_j \cos\zeta + G_j \sin\zeta) \ , \tag{9.14}$$

$$\frac{\mathrm{d}\zeta}{\mathrm{d}t} = -\Delta\omega + A\sum_{jkl}\frac{a_k a_l}{a_j}(F_j \sin\zeta - G_j \cos\zeta) \ . \tag{9.15}$$

Here, $\Delta\omega = \omega_1 + \omega_2 + \omega_3$. If there is no dissipation, Equations 9.14 and 9.15 are integrable (conserved quantity exists). If there is dissipation, they are not integrable and become chaotic. If there is a fixed point at which the system settles, it is determined by $\dot{a}_j = 0$ and $\dot{\zeta}_j = 0$.

The above discussion is the case for 2-dimensional turbulence. As is well know, there is an essential difference between 2-dimensional and 3-dimensional turbulence. As introduced in Section 9.2, a 2-dimensional turbulence structure is observed at zero magnetic shear for the electron. With magnetic shear, turbulence becomes 3-dimensional due to poloidal coupling of the modes and creates the unique structure of a streamer.

Note: 2- and 3-dimensional isotropic turbulence

Drift wave turbulence in the plasma does not have a single wave number k in the wave number space but has a spectrum in k space. If there is a driving force of the turbulence at some k region, energy flow occurs in the direction of a larger k in k space. The plasma has the characteristics of a fluid and the nonlinear term $\boldsymbol{u} \cdot \nabla \boldsymbol{u}$ in the fluid equation produces a wave with a wave number twice that of initial wave and produces energy flow toward the high k region.

The turbulence energy entering the small wave number region passes through the inertia region where dissipation is negligible and reaches the high wave number region where wave energy is dissipated as thermal energy, the dissipation region. Homogeneous isotropic turbulence is well known with a known spectrum which does not vary with translation, rotation and reflection. The spectrum of the inertia region of homogeneous isotropic turbulence is given by Kolmogorov [11] and is called the "Kolmogorov spectrum":

$$F(k) = Ck^{-5/3} \ . \tag{9.16}$$

In confined plasma, turbulence may develop perpendicular to the magnetic field because of the magnetic field. In this case, turbulence may become 2-dimensional and show quite a different character compared with 3-dimensional homogeneous isotropic turbulence:

1. Energy flow is from high k to low k, the opposite of 3-dimensional turbulence;
2. k spectrum of homogeneous isotropic 2-dimensional turbulence is $\sim k^{-3}$.

Mode Selection Rule in Three-wave Coupling [12]

If we consider the coherent three-wave interaction, it should satisfy following selection rules:

$$\omega_{\boldsymbol{k}_1} + \omega_{\boldsymbol{k}_2} = \omega_{\boldsymbol{k}} \ , \tag{9.17}$$

$$\boldsymbol{k}_1 + \boldsymbol{k}_2 = \boldsymbol{k} \ . \tag{9.18}$$

This coherent three-wave interaction becomes possible only when the structure of the dispersion curve $((k, \omega)$ is convex upward since $|\boldsymbol{k}_1 + \boldsymbol{k}_2| = |\boldsymbol{k}| \leq |\boldsymbol{k}_1| + |\boldsymbol{k}_2|$ as shown in Figure 9.7.

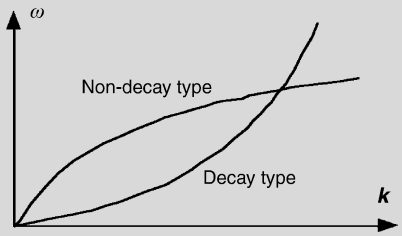

Figure 9.7 Dispersion curve of decay-type and non-decay type waves

9.4 Structure Formation: Turbulence Suppression by Shear Flow and Zonal Flow

Convective cells produced by drift wave turbulence induce heat and particle transport with a step length of the cell size. This convection cell experiences $v_E = E_r/B$ drift due to radial electric field E_r. If the magnitude of v_E changes radially, the displacement of the two edges of the cell is different and the cell is distorted and breaks down by the sheared flow as shown in Figure 9.8. The shearing rate is proportional to $\mathrm{d}v_E/\mathrm{d}r$. Poloidal rotation in a tokamak is kept small due to neoclassical viscosity, but v_E itself is not subject to this constraint and the turbulence can be suppressed by the radial electric field shear [13].

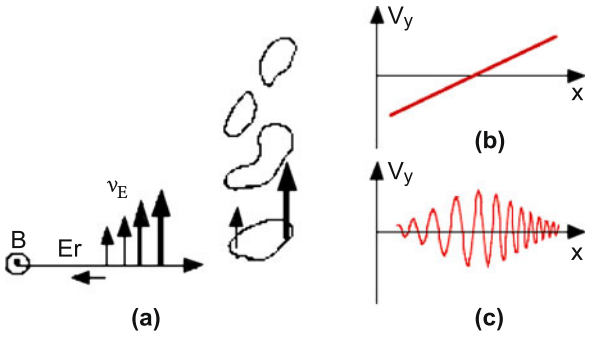

Figure 9.8 (a) Schematics of break up of the cell by the radial electric shear. (b) Schematics of the neoclassical Er shear flow balanced to pressure gradient, and (c) the zonal flow produced by turbulence [16]

While drift wave turbulence is formed by the interaction of a broad wave spectrum, a mode with $m = n = 0$, $k_{//} = 0$ can be created in ITG turbulence or ETG/TEM turbulence in the case of zero magnetic shear through the interaction of similar wave numbers. This is called "zonal flow." According to Rosenbluth–Hinton [14], the zonal flow can remain in a collisionless plasma and suppress the level of turbulence. When potential fluctuation in an $m = n = 0$ mode coupled with $m = 1$, $n = 0$ mode of the toroidal effect, a low frequency oscillation called "GAM (Geodesic Acoustic Mode)" appears. This mode is observed when the safety factor q is high [15].

The production mechanism of zonal flow is different between ions and electrons. As mentioned in the Section 9.3, electron turbulence becomes 2-dimensional in a weak magnetic shear and zonal flow is created if a density gradient exists [3]. However, it becomes 3-dimensional with a magnetic shear and the zonal flow becomes difficult to produce. On the other hand, in ITG turbulence, the zonal flow is also produced with the magnetic shear. In a tokamak, the drift wave also has the structure of the ballooning eigen function from the constraints of the double-periodic boundary conditions. Uniform amplitude approximation (see Section 6.6) holds for the pump wave of drift wave turbulence as follows,

$$\tilde{\Phi}_0(\boldsymbol{x}, t) = \exp(-\mathrm{i}n\zeta - \mathrm{i}\omega_0 t) \sum_m \tilde{\varphi}_0(m - nq) \exp(\mathrm{i}m\theta) + \text{c.c.} \tag{9.19}$$

Then, zonal flow ($\tilde{\Phi}_{\mathrm{ZF}}$) and side bands ($\tilde{\Phi}_+$ and $\tilde{\Phi}_-$) are created by "modulational instability" [16]. Let q_{r} be the radial wave number,

$$\tilde{\Phi}_{\mathrm{ZF}}(\boldsymbol{x}, t) = \exp(\mathrm{i}q_r r - \mathrm{i}\Omega t)\tilde{\varphi}_{\mathrm{ZF}} + \text{c.c.}\,, \tag{9.20}$$

$$\tilde{\Phi}_+(\boldsymbol{x}, t) = \exp(-\mathrm{i}n\zeta - i\omega_0 t + \mathrm{i}q_r r - \mathrm{i}\Omega t) \sum_m \tilde{\varphi}_+(m - nq) \exp(\mathrm{i}m\theta) + \text{c.c.} \tag{9.21}$$

$$\tilde{\Phi}_-(\boldsymbol{x}, t) = \exp(-\mathrm{i}n\zeta + \mathrm{i}\omega_0 t + \mathrm{i}q_r r - \mathrm{i}\Omega t) \sum_m \tilde{\varphi}_-(m - nq) \exp(\mathrm{i}m\theta) + \text{c.c.} \tag{9.22}$$

Growth of zonal flow is governed by the following equation:

$$\frac{\partial V_{\theta,\mathrm{ZF}}}{\partial t} = \frac{\partial}{\partial r} \langle \tilde{v}_\theta \tilde{v}_r \rangle - \gamma_{\mathrm{damp}} V_{\theta,\mathrm{ZF}}\,. \tag{9.23}$$

Here, $V_{q\mathrm{ZF}}$ is the zonal flow velocity, $\tilde{v}_\theta$ and $\tilde{v}_r$ are the poloidal and radial velocity fluctuations, γ_{damp} is the damping rate of the zonal flow. The first term of right-hand side of Equation 9.23 is called "Reynolds stress." Zonal flow and GAM are observed experimentally in toroidal plasma considered to be the main mechanism for improved confinement [17]. Since the first observation of the internal transport barrier (ITB) in JT-60 [18], formation of various ITB are observed as shown in

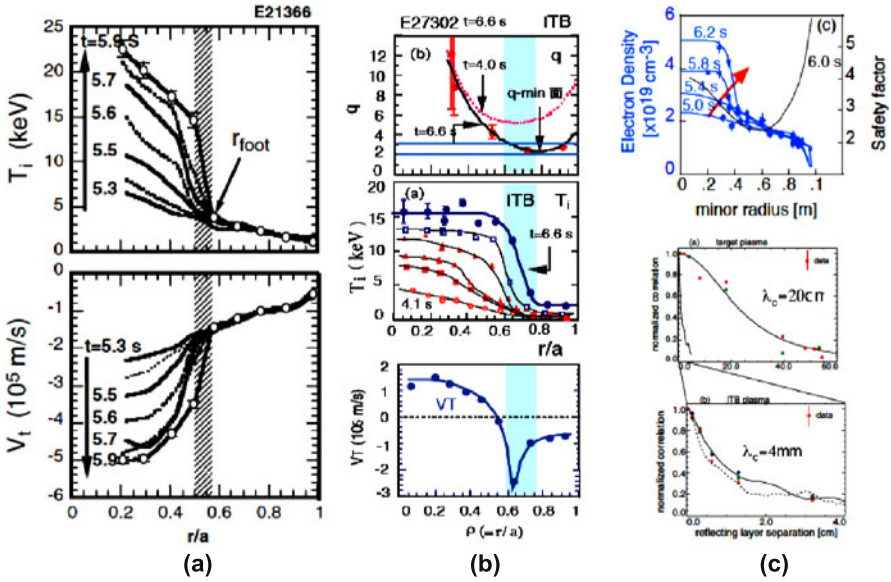

Figure 9.9 (a) Formation of ITB in the positive magnetic shear in JT-60 [19]. (b) Formation of ITB in negative magnetic shear in JT-60 [20]. (c) Measured radial correlation length before and after ITB formation [21]

Figure 9.9 [19, 20]. The long correlation length of L-mode is observed as a common characteristic of self-organized criticality [21]. It is also observed that correlation length becomes quite short due to the ITB formation. Thus, self-organized criticality is locally relaxed due to the formation of E_r shear and "structure formation" ITB occurs in the plasma.

References

1. Thompson JM and Stewart HB (1986) Nonlinear Dynamics and Chaos: Geometrical Methods for Engineers and Scientists. John Wiley & Sons Ltd.
2. Idomura Y, Tokuda S, Kishimoto Y (2005) Nucl. Fusion, 45, 1571–1581; also Idomura Y, Wakatani M and Tokuda S (2000) Phys. Plasmas, 7, 3551–3556.
3. Idomura Y (2006) Phys. Plasmas, 13, 080701.
4. Ryter F, Angioni C, et al. (2005) Phys. Rev. Lett. 95, 085001; also Ryter F, Tardini G et al. (2005) Nucl. Fusion, 43, 1396–1404.
5. Nicolis G and Prigogine I (1977) John Wiley and Sons.
6. Chandrasekhar S (1961) Hydrodynamics and Hydromagnetic Stability. Dover Books.
7. Bak P et al. (1988) Phys. Rev., A38, 364–374; also Bak P et al. (1987) Phys. Rev. Lett., 59, 381–384.
8. Hasegawa A, Mima T (1978) Phys. Fluids, 21, 87–92.
9. Hasegawa A, Wakatani M (1987) Phys. Rev. Lett., 59, 1581–1584.

10. Horton W, Ichikawa Y-H (1996) Chaos and Structures in Nonlinear Plasmas. World Scientific.
11. Kolmogorov AN (1941) Doklady Akad. Nauk SSSR, 30, 9.
12. Hasegawa A (1975) Plasma Instabilities and Nonlinear Effects. Springer-Verlag Berlin, Section 4.3 b.
13. Biglari H, Diamond PH, Terry PW (1990) Phys. Fluids, B2, 1.
14. Rosenbluth MN, Hinton F (1998) Phys. Rev. Lett., 80, 724.
15. Miyato N, Kishimoto Y, Li YJ (2007) Nucl. Fusion, 47, 929.
16. Diamond PH, Itoh S-I, Itoh K, Hahm TS (2005) PPCF, 47, R35.
17. Fujisawa A (2009) Nucl. Fusion, 49, 1.
18. Koide Y, Kikuchi M et al. (1994) Phys. Rev. Lett., 72, 3662.
19. Koide Y, Ishida S, M. Kikuchi M et al. (1994) Proc. 15th FEC, Seville, 1994, Vol. 1, 199–210.
20. Fujita T et al. (1998) Nucl. Fusion, 38, 207.
21. Nazikian R, Shinohara K, Kramer GJ et al. (2005) Phys. Rev. Lett., 94, 135002.